Journal of Marine Systems 145 (2015) 37–52

Contents lists available at ScienceDirect

Journal of Marine Systems

journal homepage: www.elsevier.com/locate/jmarsys

Inshore/offshore water exchange in the Gulf of Naples

Daniela Cianelli [a,b], Pierpaolo Falco [a], Ilaria Iermano [a], Pasquale Mozzillo [a], Marco Uttieri [a], Berardino Buonocore [a], Giovanni Zambardino [a], Enrico Zambianchi [a,*]

[a] Dipartimento di Scienze e Tecnologie, Università degli Studi di Napoli "Parthenope", CoNISMa, Centro Direzionale di Napoli Isola C4, 80143 Napoli, Italy
[b] ISPRA — Istituto Superiore per la Protezione e la Ricerca Ambientale, Via Vitaliano Brancati 60, 00144 Roma, Italy

ARTICLE INFO

Article history:
Received 5 March 2014
Received in revised form 4 January 2015
Accepted 6 January 2015
Available online 10 January 2015

Keywords:
HF coastal radars
Ocean circulation
Coastal currents
Numerical models

Regional index terms:
Mediterranean Sea
Tyrrhenian Sea
Gulf of Naples

ABSTRACT

The Gulf of Naples is a coastal area in the south-eastern Tyrrhenian Sea (western Mediterranean). Zones of great environmental and touristic value coexist in this area with one of the largest seaports in the Mediterranean Sea, industrial settlements and many other pollution sources. In such an environment, water renewal mechanisms are crucial for maintaining the ecological status of the coastal waters. In this paper, we focus on the water exchange between the interior of the Gulf and the neighbouring open Tyrrhenian Sea. The surface dynamics of the Gulf have been investigated based on measurements carried out with a high-frequency (HF) radar system. The vertical component of the current field has been provided by the Regional Ocean Modelling System (ROMS) model of ocean circulation. We present the results of a one-year-long analysis of data and simulation results relative to the year 2009. Inshore/offshore exchanges were assessed by looking at the zonal component of the surface and subsurface current field across a transect representing a sort of threshold between the interior of the Gulf and the open sea. This also allows for the reconstruction of the short-term origin of waters found inside the Gulf in the different forcing and circulation conditions.

1. Introduction

Coastal areas are complex environments in which multiple factors interact and affect the water quality and environmental state of the marine ecosystem. The factors include hydrological, geomorphological, and socio-economic conditions. In this context, the Gulf of Naples (GoN), a marginal basin in the Southern Tyrrhenian Sea, is a paradigmatic coastal area because of its particular oceanographic and morphological characteristics, and because of its highly urbanized coast, heavy maritime traffic, waste water discharges, and freshwater inputs (as reviewed in Cianelli et al., 2012). In addition, the eastern part of the GoN receives runoff from the Sarno River, a tributary carrying a heavy load of pollutants, sediment, and suspended matter that can affect the physical, chemical, and biological quality of coastal waters (Montuori and Triassi, 2012). As a result, a number of contaminants can be found in the sediments, water, and biota of the GoN, with potential repercussions on human health (as recently surveyed by Tornero and Ribera d'Alcalà, 2014). Therefore, the maintenance and improvement of the environmental quality of the GoN are critical for not only the safety of the entire ecosystem, but also for social and economic reasons.

In order to sustainably manage the environmental resources of a coastal area such as the GoN, as well as to preserve and mitigate potentially hazardous events and to monitor the water quality, understanding the surface circulation and the processes that drive the coast–offshore transport in this region is crucial. The GoN coastal area has been subject to several investigations (see Cianelli et al., 2012 for a historical overview), but prior studies have been limited by the available observational techniques. Hydrological parameters have been measured in situ in the framework of distinct oceanographic surveys, shedding light on the local dynamics but with limited sampling and very little synopticity (De Maio and Moretti, 1973; De Maio et al., 1978–1979, 1983, 1985).

Biological, chemical, and hydrological samples have been collected more regularly since 1984 in the framework of the MareChiara Long-Term Ecological Research Station (LTER-MC), although with a limited spatial resolution (Mazzocchi et al., 2011, 2012; Ribera d'Alcala et al., 2004; Zingone et al., 2010). Satellite-tracked drifters can provide Lagrangian data on circulation patterns, and the GoN has been the stage of recent Lagrangian experiments (e.g., Zambianchi, unpublished data reports relative to 2009 and 2012). Coastal-based high-frequency (HF) radar systems (see Barrick et al., 1977, and Barrick, 1978, for early accounts of this technique) are a relatively novel remote sensing technique that currently represents the most suitable tool for describing and investigating the multi-scale circulation patterns in coastal areas. This technique has the potential to provide surface current observations

* Corresponding author. Tel.: +39 3296506097; fax: +39 0815476515.
E-mail address: enrico.zambianchi@uniparthenope.it (E. Zambianchi).

http://dx.doi.org/10.1016/j.jmarsys.2015.01.002
0924-7963/

with a synoptic spatial coverage that is not achievable with other methods (Barth et al., 2008).

Coastally based HF radars can capture essential processes in the coastal ocean, including wind-driven (Kosro, 2005; Kosro et al., 1997) and tidal currents (Erofeeva et al., 2003; Kurapov et al., 2003; O'Keefe, 2005). The data typically cover both shelves, where the dynamics are predominantly wind-driven, and the adjacent coastal transition zone (CTZ), where the dynamics are more dominated by nonlinear interactions of jets and eddies and fed by the coastal current instabilities and separation (Brink and Cowles, 1991; Koch et al., 2010). Combined with other measurement techniques, HF radars can thus provide essential information for the study of the surface coastal circulation and can be used in a number of applications such as oil spill response, water quality monitoring, search and rescue, and safe and efficient maritime navigation.

An HF radar system has been active since 2004 over almost the entire area of the GoN and has been used in different applications in recent years (e.g. Cianelli et al., 2013; Menna et al., 2007; Uttieri et al., 2011). Most of the HF radar-based investigations focus on relatively short periods of time (from days to weeks), and only a few use radar-derived current measurements over periods of six months or longer (e.g. Cosoli et al., 2012; Gough et al., 2010; Kaplan et al., 2005; Kovačević et al., 2004; Robinson and Wyatt, 2011; Uttieri et al., 2011). This approach allows for the determination of seasonal to annual basin dynamics (i.e. surface currents, waves, tidal currents) at unprecedented spatial and temporal resolutions. In this framework, a one-year-long HF radar time series of surface currents (from January 1 to December 31, 2009) is accompanied by the results of numerical simulations, which were used to analyse the seasonal variability of current patterns in the GoN and to better understand the three-dimensional dynamics of the flow.

To this end, an ad hoc configuration of the three-dimensional numerical ocean model ROMS (Regional Ocean Modelling System) was implemented for the study area. In particular, we assessed the existence of different seasonal inshore/offshore regimes by computing the average surface current along a transect delimiting the boundary between the inner gulf and the open sea. The paper is organised as follows. Section 2 provides a detailed description of the study area. Section 3 presents a summary of the used methods. Section 4 describes the results of the analysis, which are discussed in Section 5 along with the conclusions.

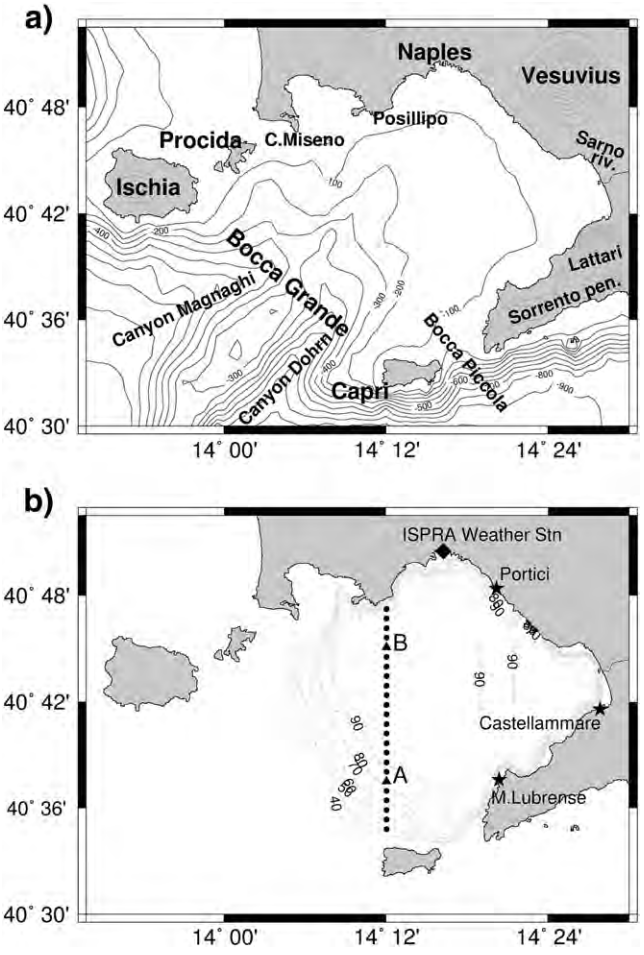

Fig. 1. a) Map of the Gulf of Naples (GoN) with bathymetry and all geographical locations mentioned in the text. b) Position of the analysed Capri–Posillipo transect with the selected points A and B; location of the three CODAR stations installed in the GoN (star symbols) and map of radar coverage percentage; location of the ISPRA weather station in the Port of Naples (diamond symbol).

2. Study area

The GoN (Fig. 1) is a semi-enclosed basin located in the south-eastern Tyrrhenian Sea (western Mediterranean). The Gulf is delimited by the Sorrento Peninsula and the island of Capri in the south and Capo Miseno and the islands of Procida and Ischia in the north. Its average depth is 170 m, and it covers an area of approximately 900 km^2 (Carrada et al., 1980). Exchanges with the adjacent basins are guaranteed by different openings (Aiello et al., 2001): with the southern Tyrrhenian Sea through the Bocca Grande (between Ischia and Capri); with the Gulf of Gaeta to the north via the shallow Ischia and Procida channels (12-m and 22-m maximum depths, respectively); and with the Gulf of Salerno to the south through the Bocca Piccola (between Capri and the Sorrento Peninsula), a sill with a depth of 74 m steeply sloping down to the 1000 m isobath. The Magnaghi and Dohrn canyons, with depths of up to 800 m, represent the main bathymetric feature of the Bocca Grande area and control the transport of sediments from the shelf to the continental slope (on the subject of vertical flows in correspondence of canyons see e.g. Canals et al., 2013). Also, local orography shows intricate features, with the Vesuvius volcano (elevation: 1281 m) and hills in the city of Naples (elevation up to 450 m) in the northern part, and the Lattari mountains (Mount Faito: 1131 m) in the south (Fig. 1a).

Several factors acting at different spatial and temporal scales drive the surface circulation in the GoN, while the deeper circulation is more directly influenced by the interaction between the currents along the water column and the complex bottom topography of the basin (Gravili et al., 2001; Grieco et al., 2005). The drivers of the surface circulation can thus be differentiated between local and remote forcings (Gravili et al., 2001).

The main local factor influencing the surface circulation of the GoN is wind (De Maio et al., 1985; Menna et al., 2007; Moretti et al., 1976–1977). Seasonal wind regimes are recognisable (Menna et al., 2007). Intense NNE–NE winds are typical of the winter season, with occasional alternations with SW winds associated with the transit of depressionary systems (Menna et al., 2007).

Owing to the deviating effect of Vesuvius and of the hills surrounding Naples, a coast–offshore jet current develops under the effect of NNE–NE winds (Cianelli et al., 2012, 2013; De Maio et al., 1983, 1985; Gravili et al., 2001; Grieco et al., 2005; Moretti et al., 1976–1977), enhancing the renewal of waters (Cianelli et al., 2013; Menna et al., 2007). In contrast, south-westerly winds induce the formation of cyclonic and anticyclonic structures, and surface currents are mostly directed towards the coast, favouring stagnation (Cianelli et al., 2013; Menna et al., 2007). In late spring and summer, the main wind regime is represented by breeze. The wind field rotates clockwise over a 24-h period as a result of the alternation of the sea-breeze (during night hours) and land-breeze (during day hours), owing to the different heat capacities of water and land (Menna et al., 2007). The absence of stronger, larger-scale wind forcing (e.g. the transit of low pressure systems) during this period of the year is typically due to the reinforcement of the Azores anticyclone, which makes this circulation scheme persistent over the entire spring–summer seasons. The circulation of the basin responds directly to this stressor, showing a consistent rotation of the surface current field over the length

of the day, with the alternation of coastward and offshore currents from the effects of sea-breeze and land-breeze, respectively (Cianelli et al., 2012, 2013; Uttieri et al., 2011).

The most prominent remote forcing mechanism is the circulation of the Southern Tyrrhenian Sea (Cianelli et al., 2012, 2013; Gravili et al., 2001; Pierini and Simioli, 1998). Its circulation is cyclonic overall, with surface Atlantic waters flowing over northern Sicily and determining a predominantly north-westward current along the western Italian coasts (Artale et al., 1994; Buffoni et al., 1997; Krivosheya and Ovchinnikov, 1973; Millot, 1987). There are steady characteristics only north of the Gulf of Naples (Rinaldi et al., 2010). In the presence of such forcing, two scenarios can be outlined for the circulation inside the GoN (De Maio et al., 1983). In the presence of a northward Tyrrhenian current, an intense surface flow enters through the Bocca Piccola and moves towards Ischia, entering the inner GoN and creating a basin-scale cyclonic gyre and an anticyclonic one in the innermost sector. When the remote forcing reverses direction, the circulation patterns in the outer sector of the GoN and over the shelf also reverse (Cianelli et al., 2012, 2013; De Maio et al., 1983).

3. Materials and methods

3.1. HF radar

HF radars have proved to be excellent tools to provide measurements of coastal currents (e.g. Barrick et al., 2012; Gurgel et al., 1999; Kaplan et al., 2005; Molcard et al., 2009; Paduan and Cook, 1997; Paduan and Washburn, 2013; Uttieri et al., 2011). They provide current fields on a spatial regular grid that are also well suited for validating coastal circulation models (e.g. Kuang et al., 2012) and for being assimilated into them (e.g. Barth et al., 2008; Breivik and Sætra, 2001). The high spatial and temporal resolution surface current data utilized in this study have been provided by such a system. In 2004, the first core of a network of HF coastal radars was installed in the GoN, permitting real-time synoptic monitoring of the surface current field at the basin scale. This system has been operated by the former Department of Environmental Sciences, now the Department of Science and Technology, of the Università degli Studi di Napoli "Parthenope" on behalf of the Centre for the Analysis and Monitoring of Environmental Risk (AMRA Scarl).

HF radars transmit an electromagnetic wave towards a target and measure the time taken by the reflected echo to return to the antenna. A coastal radar system emits electromagnetic waves in the 3–30 MHz band and uses gravity waves propagating over the sea surface as a target. When a Bragg scattering coherent resonance occurs (Crombie, 1955), the backscattered signal shows a clear peak in the signal spectrum (Barrick et al., 1977). If a surface current field is present beneath the gravity waves, the peaks in the backscattered signal will be shifted due to the Doppler effect (Paduan and Rosenfeld, 1996). Inverting this can provide information on the direction and intensity of the surface flow field. As each HF radar antenna only measures the radial component of surface velocity, at least two transceiving antennas are required (Barrick and Lipa, 1986; for a review on HF coastal radars, see Paduan and Graber, 1997).

The system installed in the GoN is a SeaSonde type manufactured by CODAR Ocean Sensors (Mountain View, California, USA). It works in the 25 MHz band and measures surface currents relative to the first 1 m of the water column. The temporal resolution of the system is 1 h, while the range is approximately 35 km from the coast. The original network installed in 2004 comprised two remote stations (in Portici and in Massa Lubrense). In this configuration, the spatial resolution was 1250 m. In 2008, a third antenna was installed in Castellammare di Stabia (see Fig. 1b), which improved both spatial coverage and resolution (1000 m).

The calibration of the system has been regularly checked over the years (this included repeated antenna pattern measurements; all data presented in this work have been processed on the basis of observed patterns). The observations accumulated in the period of operation have undergone severe quality control procedures and have been validated with truth data gathered during oceanographic cruises carried out in the GoN (e.g. Zambianchi, unpublished data reports relative to 2009 and 2012). Surface transport estimates were obtained from satellite observations (see Uttieri et al., 2011), with concomitant observations gathered by X-band radars (Serafino et al., 2012). Strong feedback was received by modelling results (Gravili et al., 2001; Grieco et al., 2005), which have greatly improved the understanding of the dynamics governing the circulation of the basin.

To estimate the response of surface currents to the different forcings and the seasonal variations in the net exchange between the interior of the GoN and the neighbouring Southern Tyrrhenian Sea, the meridional average of the total current and of the zonal component of the hourly surface currents measured by the HF radar system ($\overline{\mathscr{U}_{h_{tr}}}$ and $\overline{U}_{h_{tr}}$, respectively) were computed over a transect between the island of Capri and the hill of Posillipo. This region extends over 23 km in the meridional direction and 2 km in the zonal direction (Fig. 1b), and it is assumed as the boundary between the two sub-areas defined above (Fig. 1). The results presented in this work refer to a year-long investigation carried out in the year 2009, which was characterised in the summer by a pronounced decrease in water quality in the GoN, particularly in the SE sector (Uttieri et al., 2011). In addition, the spatial and temporal coverage in the selected year was very good, with a reduced number of data gaps, thus allowing an accurate estimate of the current regime (a map of radar coverage percentage is shown in Fig. 1b).

Surface currents were correlated with the wind blowing over the GoN. Wind measurements were derived from the dataset recorded by ISPRA (Institute for Environmental Research and Protection) in the Port of Naples (latitude 40.841 N; longitude 14.271 E; anemometric sensor height: 10 m a.m.s.l.; see Fig. 1b). The data were recorded every 10 min and are freely downloadable at http://www.mareografico.it/.

An analysis in terms of Empirical Orthogonal Functions (EOFs) was carried out in order to study the spatial pattern variability of the HF radar fields and to detect the principal modes regulating the flow across the section. EOF analysis requires the input data to be continuous. Fig. 1b shows the observation coverage percentage, which is almost constant and high (90%) in the inner part of the GoN, whereas it decreases rapidly outside it. To obtain a domain without observation gaps, two different approaches can be adopted: 1) filling the gaps over the entire domain using one of the different techniques described in the literature (e.g. Beckers and Rixen, 2003; Paduan and Shulman, 2004); and 2) reducing the domain to the area with the highest observation coverage percentage and then interpolating to obtain data for the radar grid points with no observations. First considering the target of our study (exchanges across the transect) and also that unrealistic dynamics in areas with very low coverage can be created by applying gap-filling procedures, we opted for the second option. The chosen area corresponds mostly with the 90% of coverage (Fig. 1b). The remaining gaps were filled by interpolating using the nearest points.

The EOFs were calculated by means of Singular Value Decomposition (SVD) (Jolliffe, 2002), removing the mean from the observations before applying the method. EOFs were calculated for the zonal and meridional components of the velocity and for its absolute value. Considering that the dataset spans over an entire year, EOFs were evaluated on both yearly and seasonal time scales. A scalar technique was applied to represent the EOF spatial field (e.g. Paduan and Shulman, 2004). Thus, the eigenvectors were scaled by the square roots of the corresponding eigenvalue.

3.2. ROMS-model

In addition to the radar observations, a 3D numerical model implementation was set up, and a one-year-long simulation was performed to complement surface measurements with a vertical view of the flow structure, again with a particular focus on the seasonal variability of the surface and subsurface coastal currents and the inshore/offshore exchanges. Numerical model simulations were performed using the Regional Ocean Modelling System (ROMS), a 3-D free-surface hydrostatic primitive-equation finite-difference model widely used by the scientific community for a diverse range of applications. These applications include large-scale circulation studies

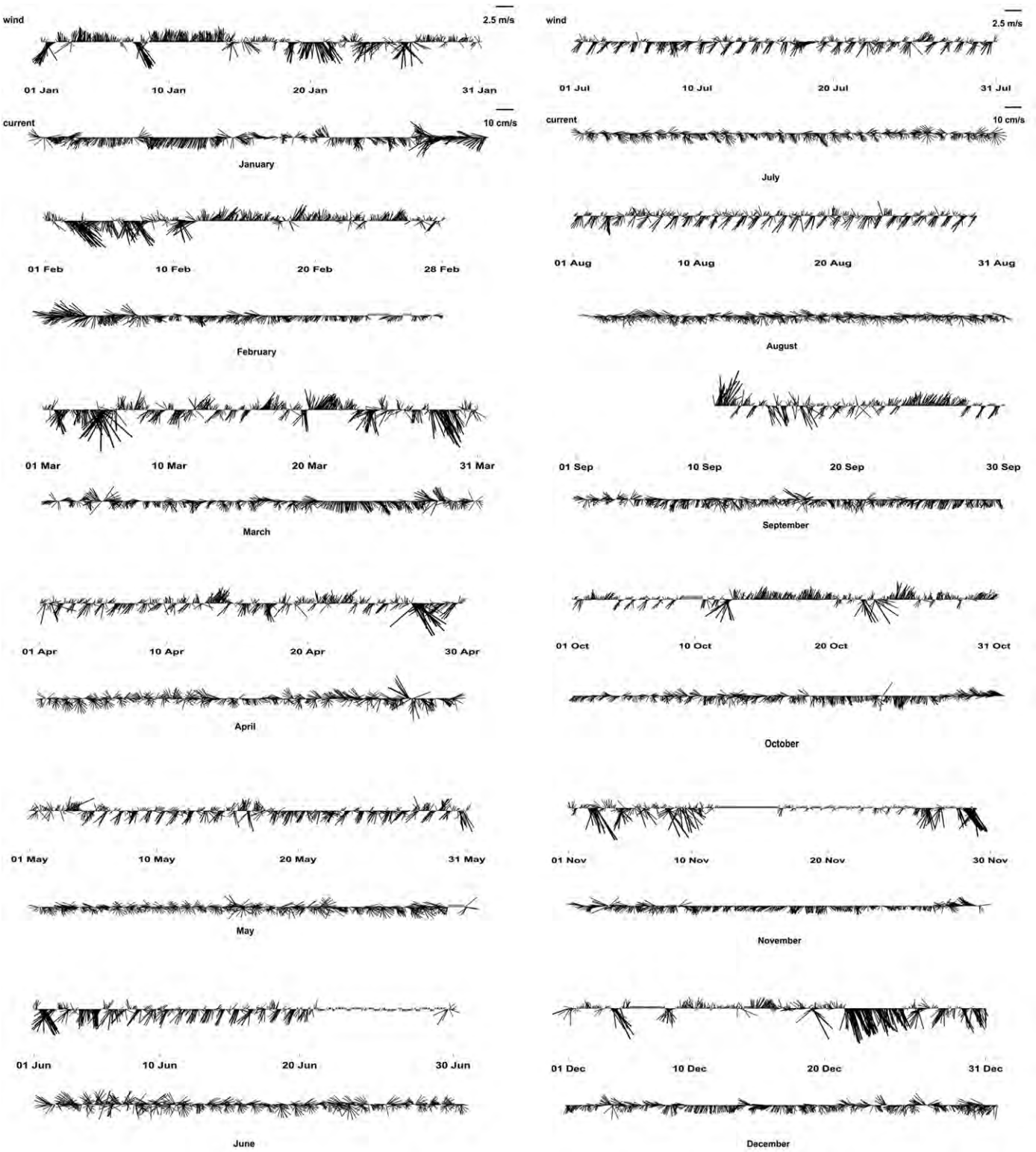

Fig. 2. Stick diagrams of the hourly average winds (m/s) measured by ISPRA in the Port of Naples (Fig. 1b) and of the HF radar surface currents (cm/s) averaged over the Capri–Posillipo transect (Fig. 1b), respectively for the periods: (left panel) January–June 2009; and (right panel) July–December 2009. Please note that, as customary, winds are plotted according to the direction from which they blow, while currents are plotted according to the direction towards which they flow.

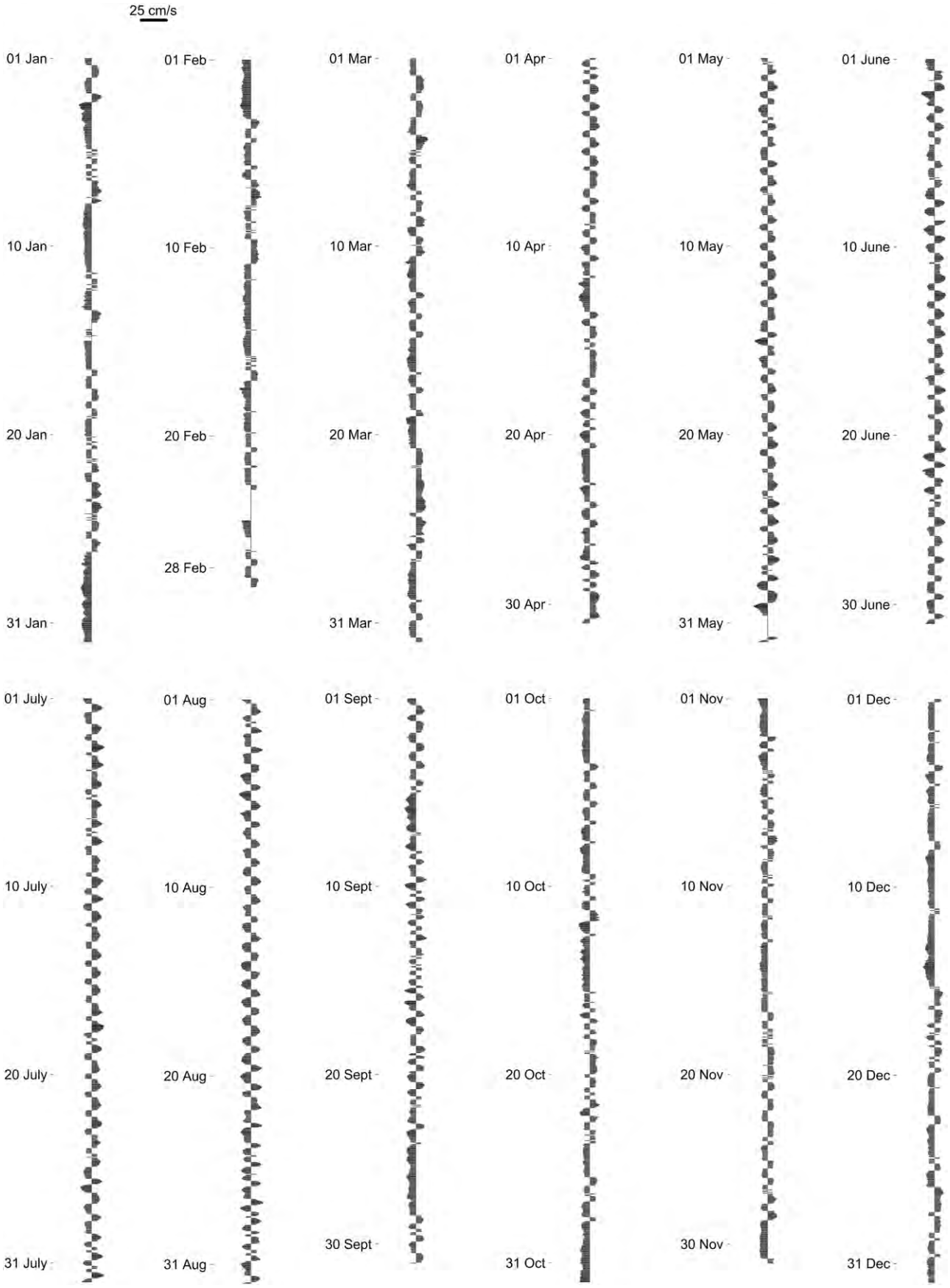

Fig. 3. Stick diagrams of the zonal component of hourly average surface currents (cm/s) measured by the HF radar for the periods: (top panel) January–June 2009 and (bottom panel) July–December 2009.

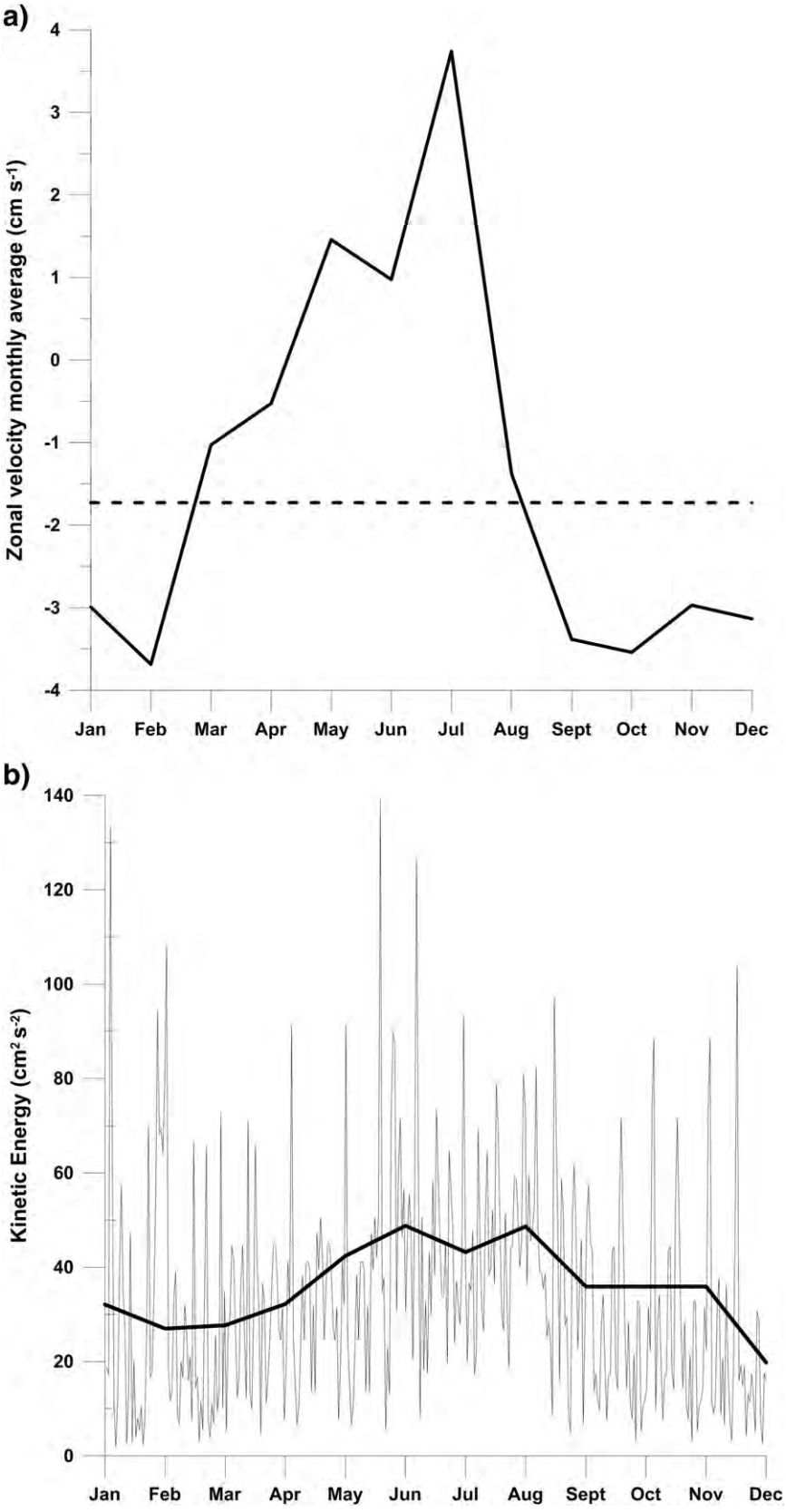

Fig. 4. (a) Time evolution of the surface current zonal component measured by the HF radar for the period January–December 2009 across the Capri–Posillipo transect: the solid line represents the monthly average, the dashed line the annual average. (b) Time evolution of the kinetic energy of the flow across the transect (i.e. of the kinetic energy computed on the zonal component of the velocity): daily average (thin line) and monthly average (thick line).

(Di Lorenzo, 2003; Haidvogel et al., 2000), polar (Budgell, 2005) and coastal oceanography (Iermano et al., 2012; Wilkin et al., 2005), biological modelling (Dinniman et al., 2003), estuary cases (Warner et al., 2005a), and operational applications (Russo et al., 2009). Details of the

ROMS computational algorithms are summarized by Shchepetkin and McWilliams (2003, 2005) and Warner et al. (2005b).

The numerical domain adopted for this study is only partially shown in Fig. 1, because it covered almost the entire coast of the Campania region, including the Gulf of Gaeta and the Gulf of Salerno. The model grid was rectangular with two solid boundaries at the northern and eastern sides and two open boundaries at the southern and western ones. The model employed a constant horizontal resolution of 1 km and a variable vertical resolution, which is enhanced at the surface and obtained using 30 σ levels. The bathymetry was derived from the General Bathymetric Chart of the Oceans (GEBCO), a global 30-arc-second database, and smoothed with a Shapiro filter to remove wavelengths on the order of the grid scale.

Vertical mixing was modelled using a two-equation second-order moment closure (k-ε) via the Generalised Length Scale (GLS) approach (Umlauf and Burchard, 2003; Warner et al., 2005b). Initial and open boundary conditions used in the numerical simulations were obtained from the daily High-Resolution Atlantic and Mediterranean Products developed by Mercator-Ocean (http://www.mercator-ocean.fr). The ROMS model was forced by SKIRON atmospheric model outputs provided by the Ocean Physics and Modelling Group and by the Atmospheric Modelling and Weather Forecasting Group of the University of Athens. The SKIRON Forecasting System is a non-hydrostatic operational model with a horizontal resolution of 0.05 × 0.05 degrees (Kallos et al., 1997), which produces hourly data of wind, air temperature, cloud coverage, relative humidity, mean sea level pressure, precipitation, and short-wave radiation. Air–sea heat and momentum fluxes are calculated by the bulk formulae of Fairall et al. (1996) using the model sea surface temperature and sea level SKIRON forcings.

The inflow of the Sarno River was included using the daily hydrometric heights obtained from the Settore Programmazione Interventi di Protezione Civile sul Territorio (the Functional Centre of the Campania Region Civil Protection Department) and subsequently transformed in the river flow through specific runoff scales. The zonal and meridional daily averaged components of the surface current derived from the ROMS model outputs were validated with the corresponding HF radar data for the entire year 2009

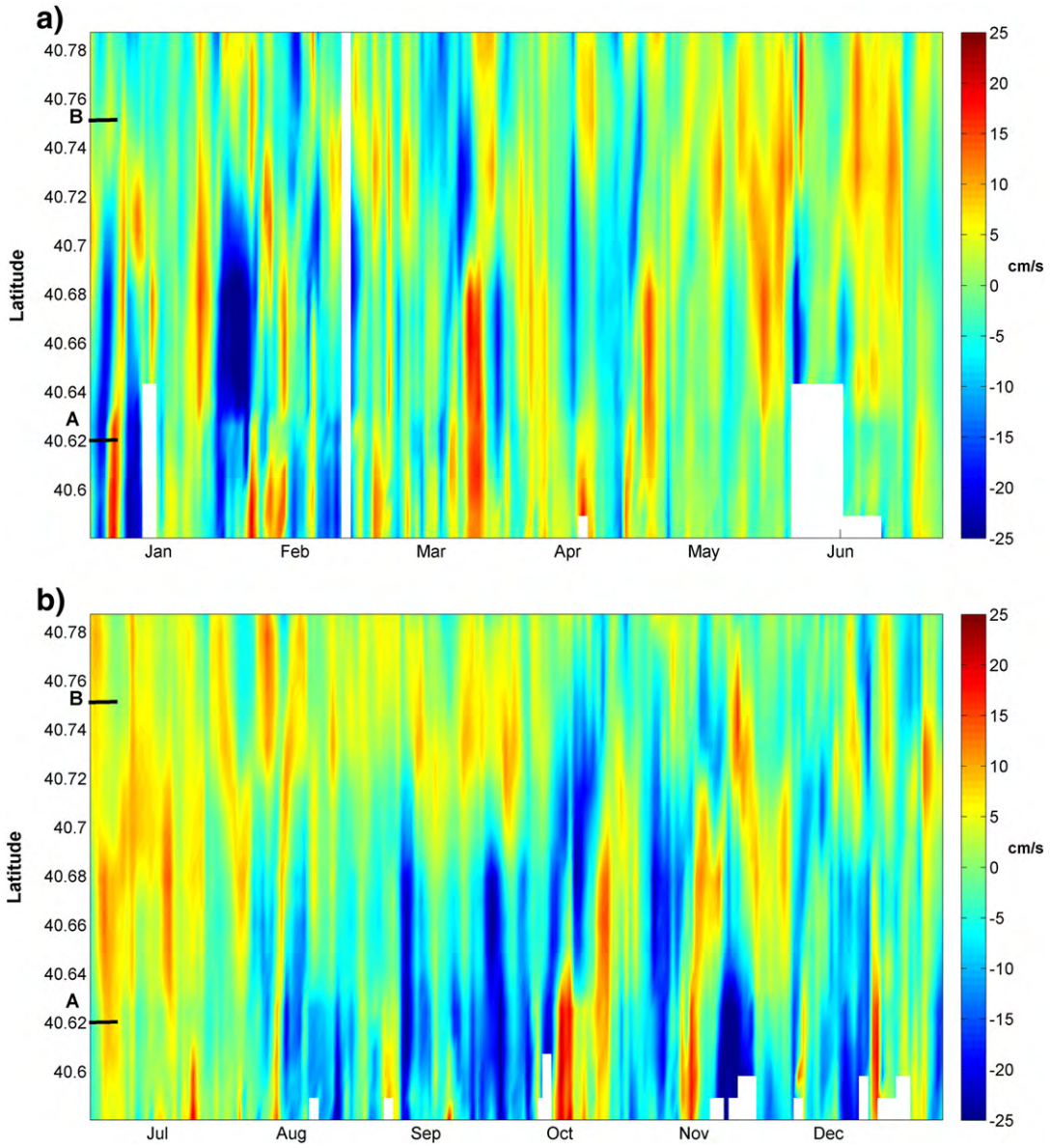

Fig. 5. Hovmöller diagrams of the zonal component of the surface current (cm/s) measured by the HF radar over the transect for the periods: a) January–June 2009 and b) July–December 2009. The latitude axis also shows the location of the two points A and B, selected so as to represent the vertical dynamics of the southern and northern part of the transect respectively (see Figs. 9 and 10).

(Appendix A). In addition, the vertical profiles of zonal flows were analysed along the selected transect through the extraction of the ROMS model grid points corresponding to two HF radar measurement positions (A: 40.625 let N, 14.201 lon E; B: 40.751 lat N, 14.201 lon E). These two points were selected to represent the respective vertical dynamics of the southern and northern parts of the transect. In particular, station A was chosen about 6 km north of Capri island in an area of approximately 200-m depth, while station B was located about 4 km south of the Posillipo coast in the north of the basin where the depth is approximately 90 m (Fig. 1b).

4. Results

4.1. Surface currents and inshore/offshore exchanges

Fig. 2 shows the winds measured by ISPRA in the Port of Naples and the mean surface currents derived from HF radar data over the analysed transect $\overline{\mathscr{U}_{h_{tr}}}$ for the entire year of 2009 (Fig. 1b). As discussed earlier, three out of the four main circulation schemes identified in the GoN (Cianelli et al., 2012, 2013) are driven by the local wind forcings. On a yearly scale, winds blowing from NE and SW usually alternated in fall and winter. There were sometimes very intense gusts, especially from the northern sectors, with speeds on the order of 5 m/s with maximum values of 9 m/s (Fig. 2). During fall and winter months, the current over the analysed transect showed a close association with the atmospheric forcing with average values of 12 and 14 cm/s, respectively.

When the wind blew from the NE sector, the current was mostly directed towards the open sea and supported by a coastal jet whose position over the basin shifted in latitude due to the deviating effect of Vesuvius (see e.g. Menna et al., 2007; Cianelli et al., 2012) (Fig. 2). In contrast, in the presence of SW winds, the mean current typically presented a marked inshore tendency. Surface waters were pulled towards the coast, thus sustaining retention and long residence times, as assessed in previous works (Cianelli et al., 2013; Menna et al., 2007) (Fig. 2). It is worth noting that there were also situations in which the wind was not the main forcing factor of the surface circulation, i.e. in the case of a strong and steady Tyrrhenian coastal current, creating a basin-scale cyclonic gyre determining a marked offshore transport (Cianelli et al., 2013; De Maio et al., 1983). Generally speaking, the wind-driven surface circulation of the GoN rapidly adapted to changes in wind direction, as evident in the first decade of January and the second decade of October and December.

In spring and summer, the main wind regime was represented by the breeze, particularly between May and September (Fig. 2). The wind field rotated clockwise over a 24-h period, as a result of the alternation of the sea-breeze (during the night) and land-breeze (during the day). For this period, the wind intensity measured by ISPRA in the Port of Naples showed average and maximum values of 2.5 m/s and 6.0 m/s, respectively. The surface dynamics of the basin responded directly to such a stressor, showing a consistent complete clockwise rotation of the current field over the length of the day, with the alternation of coastward and offshore-directed currents under the effect of sea- and land-breeze, respectively. There is an absence of stronger, larger-scale wind forcings (e.g. the transit of depressionary systems) during this period of the year due to the reinforcement of the Azores anticyclone, which makes this circulation scheme persistent over the entire spring–summer seasons. The mean current speed was 13 cm/s for both seasons.

The analysis of the zonal component of the surface currents highlighted the crucial importance of the surface forcing on the upper circulation of the GoN and showed the existence of two different prevailing patterns associated with the wind regime. During the fall and winter months, the GoN was characterised by a prevalence of an outward surface flow associated with prevailing offshore-oriented wind conditions (Fig. 3). NE winds induce a net offshore tendency of $\overline{U}_{h_{tr}}$ (Figs. 2, 3). By contrast, in the presence of SW winds, an inshore-oriented tendency of the current zonal component appeared (Figs. 2, 3).

During the spring–summer months, the GoN was characterised by alternating inflow–outflow associated with the prevalent breeze regime. Accordingly, the exchanges over the transect presented a daily alternation of inshore–offshore net movement of water, resulting in an almost balanced net flow with a slight dominance of the offshore-oriented flux (Figs. 2, 3). The seasonal character of the inshore/offshore flow is well summarized in Fig. 4a, which reports

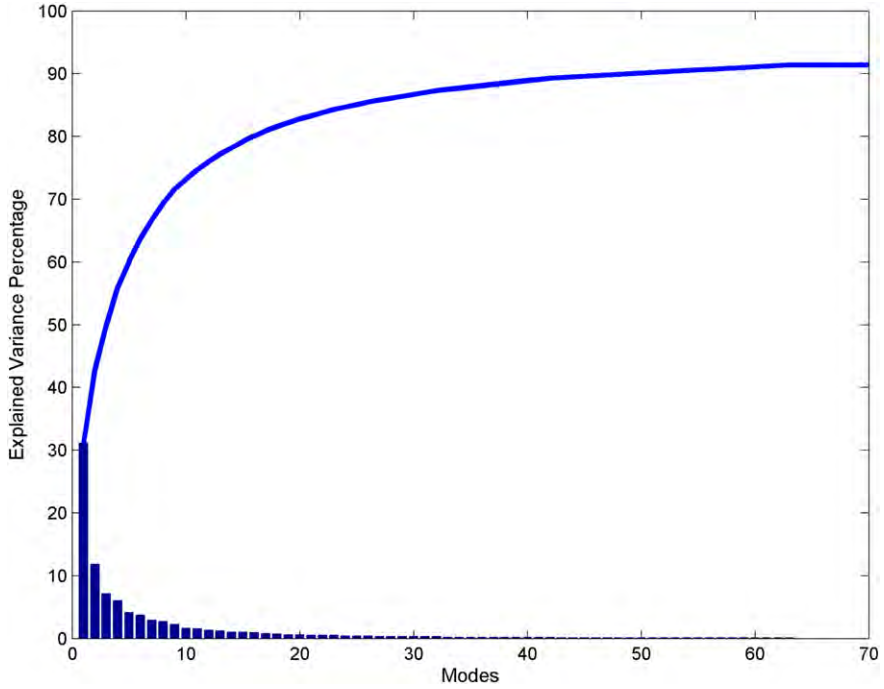

Fig. 6. Percentage of variance explained by each EOF mode (bars) and cumulative percentage (continuous line).

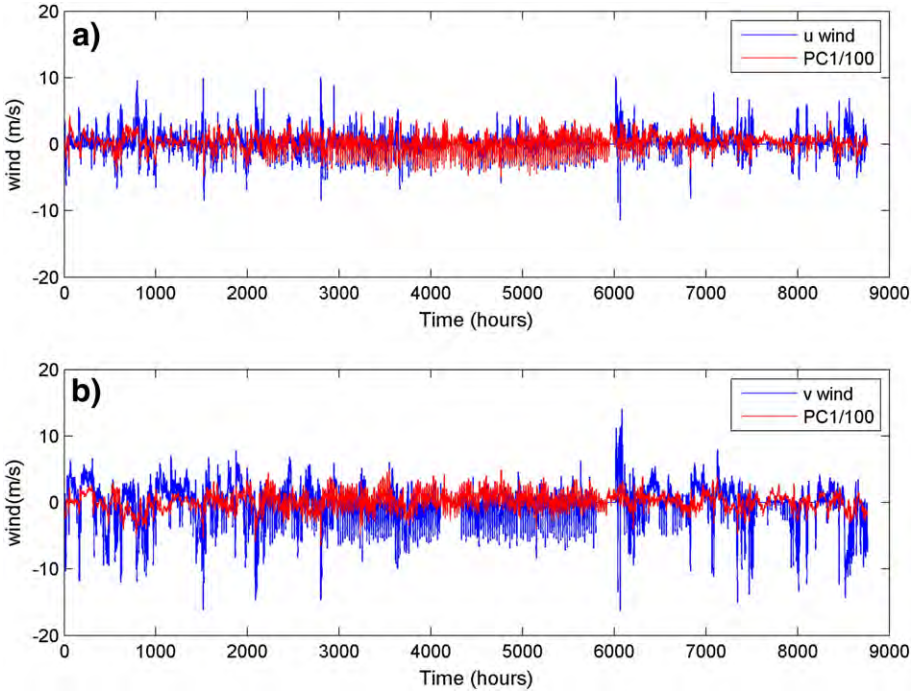

Fig. 7. Comparison between the first principal component (PC1) of the first EOF mode (red curve) and the wind (blue curve). a) Zonal wind component vs PC1 evaluated for the zonal HF radar current; and b) meridional wind component vs PC1 evaluated for the meridional HF radar current. The PC1s were scaled by a factor 100 to obtain values comparable with the wind data.

the monthly averages of the zonal component of the surface currents. Positive values indicate eastward (coastward) zonal component, whereas negative values represent westward (offshore) water flows. On a yearly average, the GoN showed a moderate tendency towards water export, as indicated by the dashed line in Fig. 4a. There is a clear seasonal dependence of the total surface flow, favouring water renewal in fall and winter and hampering it in spring and summer (more details are presented in the next section). In Fig. 4b we show the kinetic energy of the flow across the transect, which suggests the presence of a fair amount of exchange between Gulf and offshore waters and also displays some degree of seasonal variability.

4.2. Meridional detail — origin of surface waters

In order to assess the origin of waters present in the inner area of the GoN, we built Hovmöller diagrams showing the time evolution of the latitude-dependent zonal component of the surface currents measured by the HF radar system (Figs. 5a and 5b). The results show that for roughly half of the year, the zonal flow across the transect was characterised by the simultaneous presence of two opposite patterns in its northern and southern portions. On the northern side, the prevailing flow was inshore-oriented, suggesting that the northern portion of the basin was filled with waters of Tyrrhenian origin. On the southern side, the opposite condition held, implying that the southern portion of the basin was more influenced by coastal waters. However, as previously discussed, the overall pattern was strongly time-dependent, thus showing repeated and abrupt changes of sign, as well as intermingling situations of meridional coherence of the zonal flux. This general behaviour is true for part of the months of January and February, for the period of mid-August through mid-October, and from early November through mid-December. Quantitatively, this pattern typically resulted in a net outflow across the transect (see Fig. 4a), and it was more pronounced in winter and autumn with monthly $\overline{U}_{h_{tr}}$ values between −4 and −1 cm/s (where minus means westwards).

When such a two-modal distribution of zonal velocities with latitude did not occur, the variability of the wind was so frequent that the monthly averages yielded relatively small, typically inflowing values (Fig. 4a). In particular, from May to July, an inflow coming from the northern sector of the transect prevailed (Fig. 5) with monthly average values of $\overline{U}_{h_{tr}}$ between 1 and 4 cm/s. This decreased the effectiveness of the water renewal, causing stagnation and worsening the water quality in the very interior of the GoN.

To highlight the seasonal variability of the inshore/offshore exchanges, we present the EOF results aggregated in trimesters according to the wind field, which is the main surface current forcing. Looking at Fig. 2, the results of the four seasons are in agreement with the general oceanic seasonality: January–February–March are the winter months when the GoN wind field is mainly forced by the mesoscale atmospheric pressure patterns; April–May–June are the spring season characterised by post-winter and pre-summer patterns; July–August–September are summer when the wind field mainly follows the sea breeze regime; and October–November–December are the fall months.

Fig. 6 shows the amount of variance explained by each EOF relative to the current speed over the entire year of 2009. The first mode explained 33% of the total variance, the second one explained 12%, and the sum of the first four modes accounted for 56%. The first zonal and meridional component modes explained more variance than the speed first modes (48% and 46%, respectively). Considering that the wind is the main forcing of the surface circulation in the GoN (Cianelli et al., 2013; Menna et al., 2007; Uttieri et al., 2011), the first mode can be correlated with the wind field. To demonstrate this relationship, the first EOF modes of the zonal and meridional components are shown in Fig. 7 with the corresponding wind component. To compare the time variability of the first EOF modes, their expansion coefficients or principal components (PC) are represented. The PC variations are visually coherent with the local winds, confirming that these are the main driving force for the surface currents.

The surface current spatial and seasonal variability reveals several interesting features. The EOF first mode (Fig. 8) appeared to be of

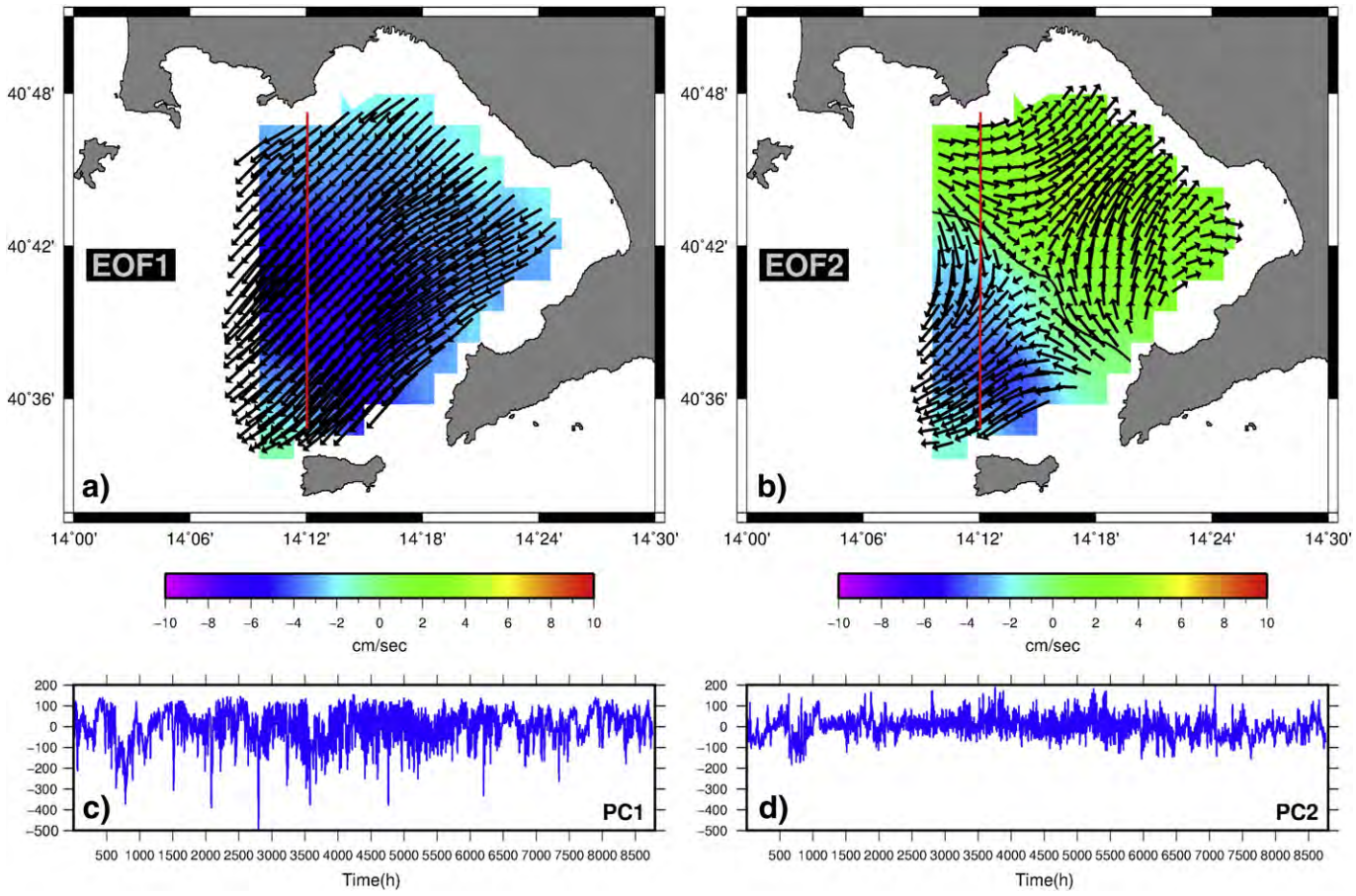

Fig. 8. 1st (a) and 2nd (b) EOF mode evaluated for the entire 2009 data set. Colours represent the spatial pattern of the current speed EOF, whereas vectors are obtained applying a scalar technique as described in Paduan and Shulman (2004). Amplitude time series for the 1st and 2nd EOF modes are shown in panels (c) and (d), respectively.

the same sign in both yearly and seasonal (not shown) evaluations. Considering that the GoN domain is relatively small, the basin responded coherently to the main wind forcing, at least over the area considered for the EOF calculations. On the other hand, restricting the domain should not influence the EOF patterns, whereas the explained variance may be lower if the entire domain is considered (Navarra and Simoncini, 2010). The first EOF mode shows a well-defined offshore-directed surface flow (Fig. 8) driven by the main local wind field. Over the whole year, the wind blows from two preferential directions in the GoN: from NE and SW (Menna et al., 2007), with the former being the most energetic one. Considering that in summer, the highly variable daily wind displays an offshore-directed component, we can argue that the first mode accounted for such flow, essentially towards offshore.

The second EOF (Fig. 8) shows a bipolar pattern with the axis aligned to the domain main axis. It is worth noting that on an annual scale, a local divergence was observed at approximately the domain centre. The second EOFs were more related to the observed exchange variability pointed out by the Hovmöller diagram shown in Figs. 5a and 5b. Such agreement is well represented by the seasonal EOF patterns, explaining 12%, 8%, 16%, and 13% of the total variance, respectively. In particular, the winter second EOF pattern (not shown) is characterised by an anticyclonic gyre which is often recognisable in the hourly HF radar current maps. The interactions with the coastal Tyrrhenian current and with the changing bottom topography were the most likely mechanisms acting to generate such recirculation.

Cyclonic gyres can also be observed in radar data (and also in past observations), both at the centre of the basin and in more coastal areas (Cianelli et al., 2013; De Maio et al., 1985). The second EOF patterns show a generally incoming flow across the northern part of the transect with the only exception in the fall, when there is an overall outflow across the section. The same general pattern was revealed by the time evolution of the zonal component over the transect (Fig. 4) and by the Hovmöller diagrams (Fig. 5). In winter, the circulation determined inflow to the north and outflow to the south of the section, which is in good agreement with the results discussed in the previous sections (Figs. 4 and 5).

4.3. The subsurface and deep inshore/offshore exchanges

ROMS numerical simulations were used in order to shed light on the vertical structure of the velocity field. Also, for the subsurface flow, our results are summarized in Hovmöller diagrams for the zonal component of the velocity field, but differently from Figs. 5a and 5b. In this case, the y-axis corresponds not to latitude but to depth (Figs. 9 and 10). As detailed above, we show results for two points on the Capri–Posillipo transect (A and B, Fig. 1b), representative of the southern and northern sectors of the transect, often been characterised by different surface regimes (see previous section).

In all points along the southern part of the transect (represented here by station A) and up to about 40.7 degrees latitude, the flow appeared mainly outgoing for most of the year at both the surface and along the water column (Fig. 9). In particular, the vertical profile of the flow showed a tendency to leave the inner part of the GoN, especially in the last months of the year (from September to December). In late winter and spring, data showed an opposite tendency of the upper water column, although considerably weaker and confined to a shallower portion of the water column. This was mirrored in the first

half of February by the surface signal of HF radar showing a very strong incoming flow for the southern points of the transect (Fig. 5a). The same signal was also found in the vertical profiles represented by station A in a very clear way up to a depth of approximately 25–30 m (Fig. 9a).

Along the northern points of the transect, from the edge of about 40.7 degrees latitude represented by station B, there was a greater variability in the exchange mechanisms and therefore a more pronounced alternation of outgoing and incoming flow throughout the year. This characteristic was evident at both the surface (Fig. 5) and along the vertical (Fig. 10). A common behaviour was observed during summer months dominated by the breeze regime (late April–August) and along almost the entire transect, i.e. a discrepancy between an incoming surface flow. This is shown by the HF radar data analysis (Fig. 5) and a tendentially outgoing subsurface flow below the first few metres down to about 60-m depth (Figs. 9 and 10). This suggests that stronger stratification is accompanied by a more pronounced baroclinic behaviour, as could be expected.

5. Discussion

In the literature, most of the HF-radar-based investigations focus on relatively short periods of time. In contrast, in the present work, a one-year-long HF radar time series is used for the first time to analyse the basin-scale seasonal variability of surface current patterns in the GoN and the associated inshore/offshore exchanges with the neighbouring Southern Tyrrhenian Sea. The observations are backed up by results of numerical simulations of the coastal circulation carried out using a specific implementation of ROMS, which provides a view of the vertical structure of the flow field not otherwise detectable through HF radar.

The comparison between wind and surface current data along a transect separating the inner part of the GoN and the open sea shows the crucial importance of the wind forcing on the upper circulation and consequently on the connectivity of this coastal basin with the Tyrrhenian Sea at the surface level. In autumn and winter, the hourly averaged current over the transect used in this work $\overline{v_{h_{tr}}}$ shows a close association with the atmospheric forcing. When winds blow from the NE sector, the current is mostly directed towards the open sea (Fig. 2), while under the action of SW winds, surface currents are coastward oriented (Fig. 3). On occasion, when the Tyrrhenian forcing becomes prevalent, this wind-driven regime is no longer observed (Cianelli et al., 2013). By contrast, in the breeze regime that is typical of late spring–summer conditions, there is an alternation of sea and land breeze blowing over the basin, to which the GoN responds with a clockwise rotation of the surface current field following the breeze daily evolution (Fig. 2).

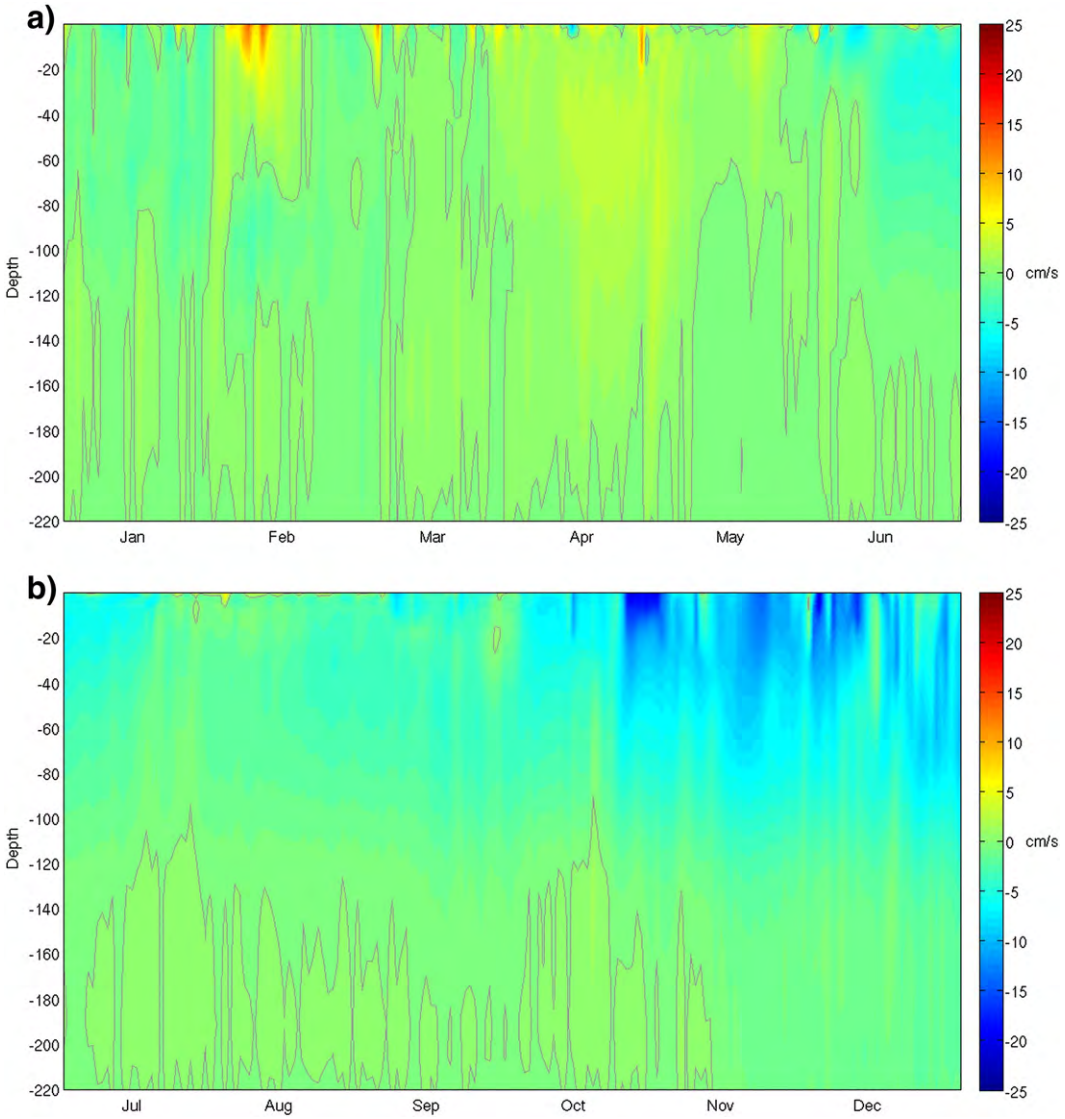

Fig. 9. Hovmöller diagrams of the daily average zonal component of the current velocity at point A (see Fig. 1) for the period: a) January–June 2009; b) July–December 2009.

The analysis of the zonal component of currents $\overline{U}_{h_{tr}}$ (Fig. 3) allows for the assessment of the existence of two different water inflow and outflow regimes in the GoN, with a tendency towards stagnation inside the basin during spring and summer and a more effective water renewal mechanism in fall and winter under NE winds. The renewal of coastal waters in spring and summer is inhibited, and the exchanges between coastal areas and open waters are hampered, with long residence times of particles released in the innermost sector of the basin (Cianelli et al., 2013; Uttieri et al., 2011). Winds originating from the northern sector cause the convergence of water along the Naples coast and the subsequent creation of an offshore directed current. This condition favours the renewal of coastal waters and the exchange between the interior of the GoN and the neighbouring Tyrrhenian Sea (Cianelli et al., 2012, 2013; De Maio et al., 1983, 1985; Menna et al., 2007; Moretti et al., 1976–1977). An opposite pattern is associated with south-westerly winds: surface waters are oriented towards the coast, which a condition sustaining retention and long residence times verified in previous works (Cianelli et al., 2013; Menna et al., 2007). The Tyrrhenian coastal current driving instead promotes an offshore zonal current sustaining the renewal of coastal waters (Cianelli et al., 2013). The EOF pattern confirms a year-round overall prevailing offshore-oriented surface current pattern described by their first mode, with a more spatially complex second mode superimposed onto it.

The pattern of in- and outflow results appear to be not only time- but also latitude-dependent. Quite often, data and simulation results show a bimodal distribution of the zonal component of the flow, resulting in the simultaneous presence of inshore and offshore currents associated with the presence of basin- and subbasin-scale structures of the flow field.

In the lower part of the transect, an offshore flux is prevalent on a yearly scale, and there is a strong correlation between the surface and subsurface flow dynamics from late summer to early winter. From late spring to early summer, the coexistence of incoming surface flow and outgoing subsurface flow confirms the influence of breeze regimes on the stagnation tendency of GoN surface waters.

The northern part of the transect exhibits a great variability of outgoing and incoming flow throughout the year and a more pronounced discrepancy between surface and subsurface flows, especially during summer months dominated by the breeze regime, with an incoming surface flow almost opposite to an outgoing subsurface flow. Furthermore, the analysis of the 2009 HF radar time series points out that on a yearly scale, the annual average flow along the chosen boundary transect is mainly outgoing, while an ingoing flow only dominates from the late spring to the summer when the maximum values are reached.

The information about the vertical profile of currents provided by numerical simulations highlights a strong coupling along the vertical,

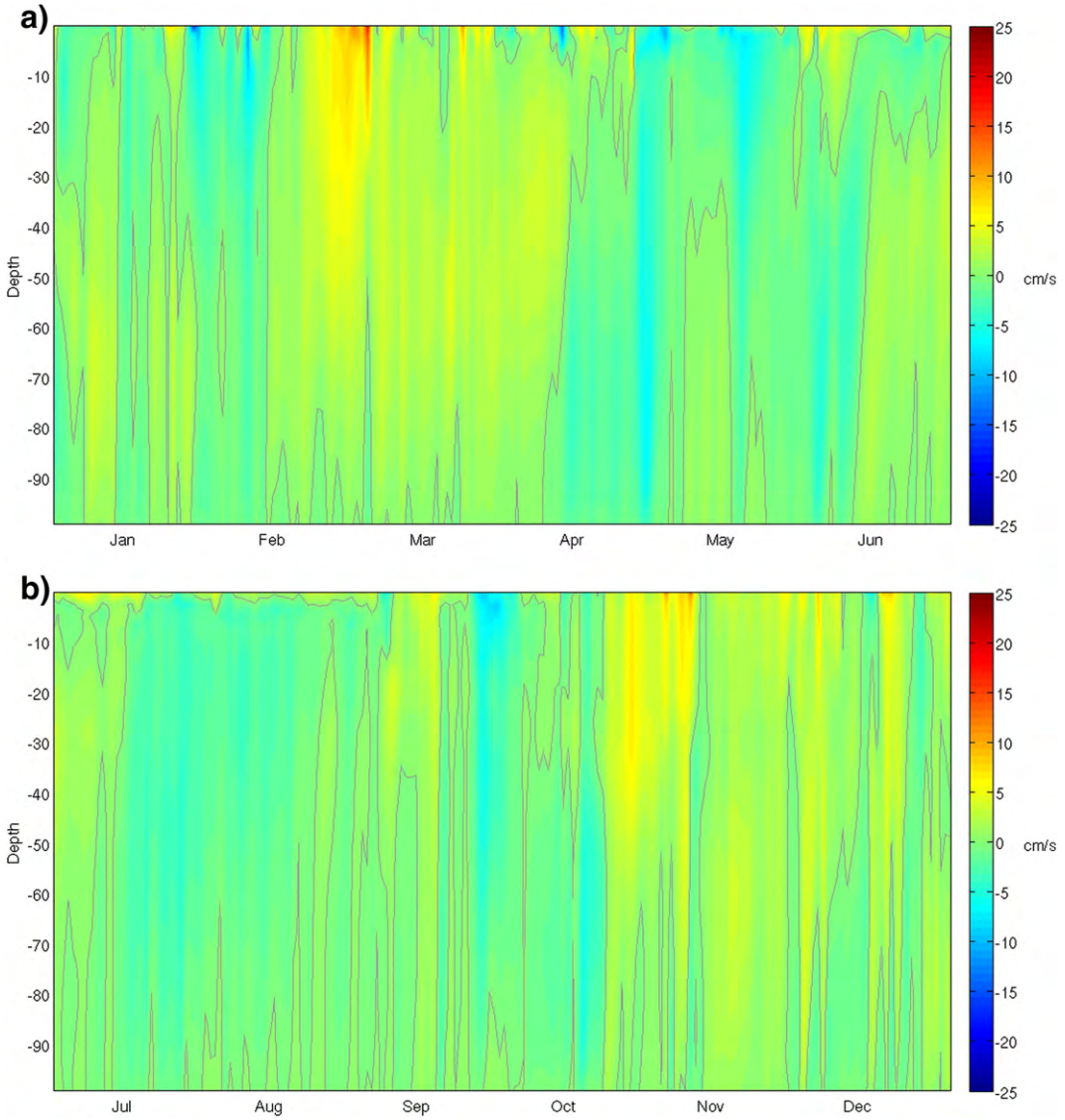

Fig. 10. Hovmöller diagrams of the daily average zonal component of the current velocity at point B (see Fig. 1) for the period: a) January–June 2009; and b) July–December 2009.

as can be expected, in shallower portions of the GoN and in seasons with weaker stratification. A stronger stratification was seen to induce a more pronounced baroclinicity. The analysis of a one-year-long time series of surface currents highlights that water exchanges between the inner and outer sectors of the GoN may also be promoted by the basin circulation scheme driven by the offshore Tyrrhenian current, in which wind conditions play only a minor role. The results of the present investigation can be complemented with a description of the biological dynamics of the basin to understand the interplay between marine circulation and plankton patterns. Two coexisting sub-systems can be identified in the GoN: the coast, featuring typical eutrophic conditions and subject to human pressure and riverine/land runoff, and the open waters with more pronounced oligotrophic characteristics (Carrada et al., 1980, 1981; Marino et al., 1984; Ribera d'Alcalà et al., 2004; Zingone et al., 1990, 1995). They are divided by a narrow boundary positioned in the coastal area in summer, and large boundary shifted towards the open sea in winter (Carrada et al., 1980, 1981; Marino et al., 1984). The inshore/offshore mechanisms highlighted in the present work (Fig. 4) support these findings, showing that in summer, the more pronounced inflow along the transect confines coastal waters and pushes the boundary between the two subsystems eastward, whereas in winter, the outflow tendency moves this boundary westward.

The connection between these two sub-systems is strongly influenced by the local circulation (Casotti et al., 2000; Cianelli et al., 2013; Menna et al., 2007). In a multiannual investigation at the LTER-MC site, Mazzocchi et al. (2011 and 2012) gave evidence for the presence of typical offshore zooplanktonic organisms in the coastal area of the GoN in winter and early spring, while in summer, only few species representative of the coastal area dominate the zooplankton assemblage. In particular, Mazzocchi et al. (2012) outlined that the copepod assemblage is poorly diversified in summer owing to coastal retention, which is in full agreement with the outcomes from the HF radar measurements and the ROMS simulations indicating a reduced exchange in this period of the year. The wintertime presence of offshore zooplankton species has been justified by a supposed entrapment in the surface circulation of the Tyrrhenian Sea (Mazzocchi et al., 2011, 2012). Considering the latitudinal proximity of LTER-MC to point B of our work, our results indicate that the proposed entrance mechanism might be valid when taking into account the surface inshore/offshore exchanges in the northern part of the GoN (Fig. 5). However, ROMS simulations provide an alternative mechanism: the more pronounced coastward orientation of subsurface currents might be an effective vector of ingression of offshore species, having a temporally more stable pattern than the surface field.

6. Conclusions

The identification of the prevailing mechanisms in the surface circulation of the GoN represents a key factor to understand the effectiveness of the exchange between coastal and offshore areas and to address issues on the water quality of such an environmentally vulnerable basin. With this goal, a one-year-long HF radar time series of surface currents was analysed and integrated with ROMS three-dimensional numerical simulations for the study area. The results underline the extraordinary value of HF coastal radars, which have the unique characteristic of providing synoptic data with high spatial and temporal resolution over coastal areas. This enables detailed understanding of the local dynamics and the pattern of local or remote forcing, which may greatly benefit from complementing these data with the three-dimensional view provided by a numerical model. The analysis of the direct relationship between wind and HF radar data showed the crucial importance of the surface forcing on the upper circulation of the GoN, while ROMS modelling outputs gave us the possibility to investigate the subsurface dynamics in more detail through the analysis of vertical profiles along the transect. Taken together, these results outline the forcing-dependent seasonally-variable exchanges between the interior of the GoN and the Southern Tyrrhenian Sea. Furthermore, they provide important details to understand the connection of the coastal system with the open sea.

Acknowledgements

The Department of Sciences and Technologies (formerly the Department of Environmental Sciences) of the University of Naples "Parthenope" operates the HF radar system on behalf of the AMRA consortium (formerly CRdC AMRA), a Regional Competence Centre for the Analysis and Monitoring of Environmental Risks. Our radar remote sites are hosted by the ENEA Centre of Portici, the "Villa Angelina Village of High Education and Professional Training", "La Villanella" resort in Massa Lubrense, and the Fincantieri shipyard in Castellammare di Stabia, whose hospitality is gratefully acknowledged. Our work was partly funded by the MED TOSCA project and by the Flagship Project RITMARE – The Italian Research for the Sea – coordinated by the Italian National Research Council and funded by the Italian Ministry of Education, University, and Research, within the National Research Program 2011–2013. The authors gratefully acknowledge the Functional Centre "Settore Programmazione Interventi di Protezione Civile sul Territorio" of the Civil Protection Department of the Campania Region for providing Sarno River runoff data, as well as the Atmospheric Modelling and Weather Forecasting Group (AM&WFG) and the Institute of Accelerating Systems and Applications (IASA) of the National and Kapodistrian University of Athens for the atmospheric data. The authors gratefully acknowledge two anonymous reviewers and the editor Dr. E. Hofmann for constructive exchanges.

Appendix A

ROMS model outputs were validated through comparison of the daily averaged surface currents with the corresponding HF radar data for the entire year of 2009. We identified the numerical model grid points closest to those of the analysed transect (Fig. 1b), and then we computed their spatial average in order to assess the temporal variability for the year 2009. All analyses were based on a depth of 1 m because the radar estimates (for a 25 MHz system like that employed in the GoN) represent average currents in the upper 50 cm to 1 m of the water column.

The time-series currents at 1-m depth for the u and v components are shown in Fig. A.1 for the period of January through December, and some evaluation metrics are provided in Table A.1. Taylor diagrams are shown in Fig. A.2. In the zonal direction, quite rapid current fluctuations are observed at these locations with a time scale of about 1 week in both datasets. In the meridional direction, stronger current amplitude episodes are observed. The comparison between model results and measured data in terms of velocities at 1-m depth shows good agreement between the ROMS model results and HF radar data, despite the numerical simulation having been conducted without any data assimilation. The ROMS model simulations are able to follow the observations closely, and the main error contribution is from amplitude mismatches (Fig. A.1).

Comparisons of modelled currents and those estimated from the HF radar are summarized in Fig. A.2 with Taylor diagrams. Taylor diagrams provide a concise statistical summary of how closely the model results match with observations (Taylor, 2001). These diagrams show the correlation coefficient (which is computed after removing the overall means) and root-mean-square difference between two fields (which is normalised by the standard deviation of the observed field), along with the ratio of the standard deviations

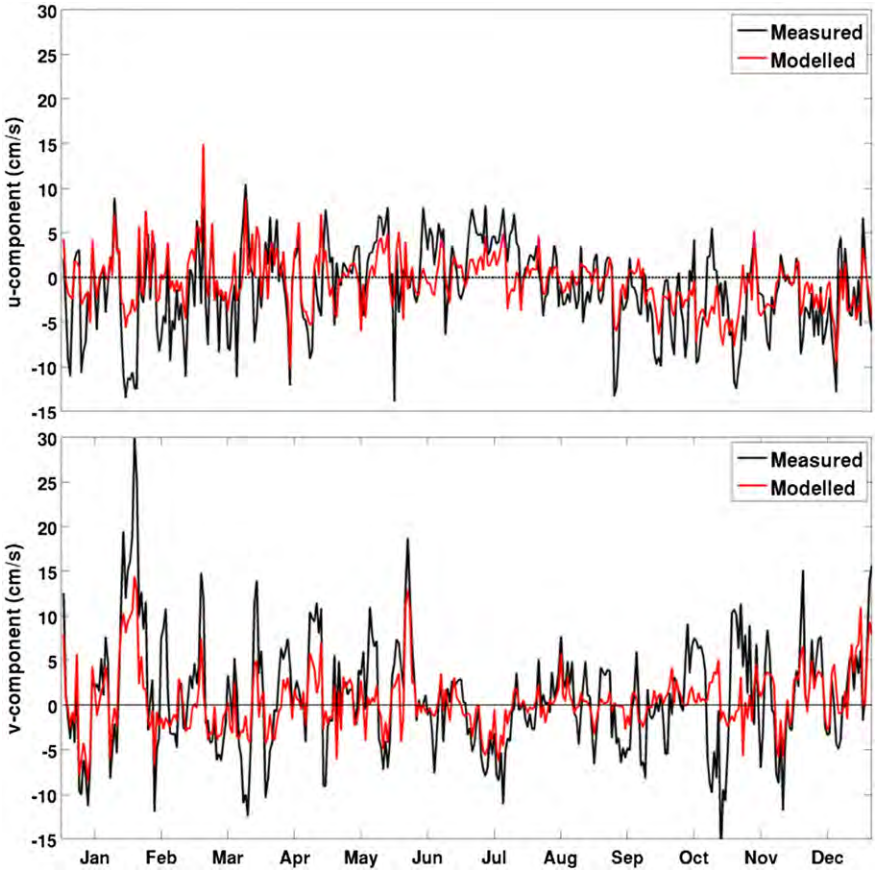

Fig. A.1. Time series of (top panel) u and (bottom panel) v surface velocity components: daily average of the HF radar data (black line) and numerical model (red line).

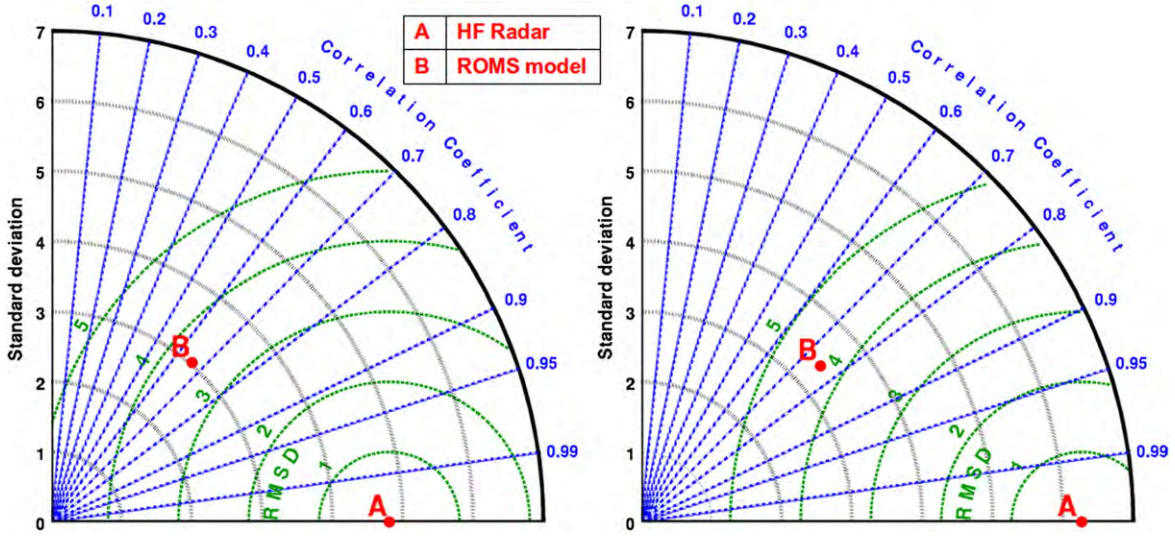

Fig. A.2. Taylor diagrams displaying pattern statistics between the HF radar observed and ROMS model fields, for the u and v velocity components (left and right panel, respectively).

Table A.1
Results of the statistical comparison between surface currents measured by the HF radar and produced by the circulation model along the transect Capri–Posillipo (Fig. 1b).

	u-Current	v-Current
Centred root mean square difference (cm/s)	3.6	4.3
Correlation coefficient	0.66	0.75

of the two patterns indicated by a single point on a two-dimensional plot. The plot is constructed based on the Law of Cosines. The radial distances from the origin to the points are proportional to the pattern standard deviation, and the cantered RMS difference between the test and reference field is proportional to their distance apart (in the same units as the standard deviation). The correlation between the two fields is given by the azimuthal position of the test field. The error metrics given in the diagrams are carried out for both model-generated currents and observations considering the latter as reference point.

In the present diagrams, the distances of model fields from the observations are relatively short for both the u and v velocity components, showing good agreement between the simulated and observed fields (Fig. A.2). In particular, they show that the current RMS difference is quite low for both the u and v velocity components (~4 cm/s), and the correlation is higher for the meridional than for the zonal velocity (Table A.1). This confirms that the main source of error of the model representation is in the amplitude of the current, as previously verified through the time-series representation (Fig. A.1).

The mismatches in the amplitude of the model currents can be attributed to various issues. First of all, in the ROMS simulations, tides were not included, even though we considered daily averaged data, and the observed time series includes a relatively weak tidal signal. Furthermore, the wind derived from models can often be underestimated due to the spatiotemporal averaging of the fields (removing wind gust velocities and small/medium scale patterns). It was found that in the Mediterranean Sea, most datasets underestimate the winds (Cavaleri, 2005; Menna et al., 2007), and no bias/correction term in the wind field was used in current numerical simulations.

References

Aiello, G., Budillon, F., Cristofalo, G., D'Argenio, B., de Alteriis, G., De Lauro, M., Ferraro, L., Marsella, E., Pelosi, N., Sacchi, M., Tonielli, R., 2001. Marine Geology and Morphobathymetry in the Bay of Naples (South-eastern Tyrrhenian Sea, Italy). In: Faranda, F.M., Guglielmo, L., Spezie, G. (Eds.), Mediterranean Ecosystems — Structures and Processes. Springer–Verlag, Berlin, pp. 1–8.

Artale, V., Astraldi, M., Buffoni, G., Gasparini, G.P., 1994. Seasonal variability of gyre-scale circulation in the northern Tyrrhenian Sea. J. Geophys. Res. 99 (C7), 14127–14137.

Barrick, D.E., 1978. HF radio oceanography — A review. Bound.-Layer Meteorol. 13, 23–43.

Barrick, D.E., Lipa, B.L., 1986. An evaluation of least-squares and closed-form dual-angle methods for CODAR surface-current applications. IEEE J. Ocean. Eng. OE-11, 322–326.

Barrick, D.E., Evans, M.W., Weber, B.L., 1977. Ocean surface currents mapped by radar. Science 198, 138–144.

Barrick, D., Fernandez, V., Ferrer, M.I., Whelan, C., Breivik, Ø., 2012. A short-term predictive system for surface currents from a rapidly deployed coastal HF radar network. Ocean Dyn. 62, 725–740.

Barth, A., Alvera-Azcárate, A., Weisberg, R.H., 2008. Assimilation of high-frequency radar currents in a nested model of the West Florida Shelf. J. Geophys. Res. 113, C08033.

Beckers, J.M., Rixen, M., 2003. EOF calculations and data filling from incomplete oceanographic datasets. J. Atmos. Ocean. Technol. 20, 1839–1856.

Breivik, Ø., Sætra, Ø., 2001. Real time assimilation of HF radar current into a coastal ocean model. J. Mar. Syst. 28, 161–182.

Brink, K.H., Cowles, T.J., 1991. The Coastal Transition Zone program. J. Geophys. Res. 96, 14637–14647.

Budgell, W.P., 2005. Numerical simulation of ice–ocean variability in the Barents Sea region. Ocean Dyn. 55, 370–387.

Buffoni, G., Falco, P., Griffa, A., Zambianchi, E., 1997. Dispersion processes and residence times in a semi-enclosed basin with recirculating gyres: an application to the Tyrrhenian Sea. J. Geophys. Res. 102 (C8), 699–713.

Canals, M., Company, J.B., Martín, D., Sànchez-Vidal, A., Ramírez-Llodrà, E., 2013. Integrated study of Mediterranean deep canyons: novel results and future challenges. Prog. Oceanogr. 118, 1–27.

Carrada, G.C., Hopkins, T.S., Bonaduce, G., Ianora, A., Marino, D., Modigh, M., Ribera d'Alcalà, M., Scotto di Carlo, B., 1980. Variability in the hydrographic and biological features of the Gulf of Naples. Mar. Ecol. 1, 105–120.

Carrada, G.C., Fresi, E., Marino, D., Modigh, M., Ribera d'Alcalà, M., 1981. Structural analysis of winter phytoplankton in the Gulf of Naples. J. Plankton Res. 3, 291–314.

Casotti, R., Brunet, C., Aronne, B., Ribera d'Alcalà, M., 2000. Mesoscale features of phytoplankton and planktonic bacteria in a coastal area as induced by external water masses. Mar. Ecol. Prog. Ser. 195, 15–27.

Cavaleri, L., 2005. The wind and wave atlas of the Mediterranean Sea — the calibration phase. Adv. Geosci. 2, 255–257.

Cianelli, D., Uttieri, M., Buonocore, B., Falco, P., Zambardino, G., Zambianchi, E., 2012. Dynamics of a very special Mediterranean coastal area: the Gulf of Naples. In: Williams, G.S. (Ed.), Mediterranean Ecosystems: Dynamics. Management and Conservation. Nova Science Publishers, Inc., New York, pp. 129–150.

Cianelli, D., Uttieri, M., Guida, R., Menna, M., Buonocore, B., Falco, P., Zambardino, G., Zambianchi, E., 2013. Land-based remote sensing of coastal basins: use of an HF radar to investigate surface dynamics and transport processes in the Gulf of Naples. In: Alcântara, E. (Ed.), Remote Sensing: Techniques. Applications and Technologies. Nova Science Publishers, Inc., New York, pp. 1–30.

Cosoli, S., Gačić, M., Mazzoldi, A., 2012. Surface current variability and wind influence in the northeastern Adriatic Sea as observed from high-frequency (HF) radar measurements. Cont. Shelf Res. 33, 1–13.

Crombie, D.D., 1955. Doppler spectrum of sea echo at 13.56 Mc./s. Nature 175, 681–682.

De Maio, A., Moretti, M., 1973. Contributo a un progetto di studio delle correnti del Golfo di Napoli. Fondazione Politecnica per il Mezzogiorno d'Italia — Quaderno n. 71.

De Maio, A., Moretti, M., Sansone, E., Spezie, G., Vultaggio, M., 1978–1979. Dinamica delle acque del Golfo di Napoli (Aprile, Settembre, Ottobre 1977). Diffusione delle acque dolci che pervengono nel Golfo. Ann.Ist. Univ. Nav. XLVII–XLVIII, 201–213.

De Maio, A., Moretti, M., Sansone, E., Spezie, G., Vultaggio, M., 1983. Dinamica delle acque del Golfo di Napoli e adiacenze. Risultati ottenuti dal 1977 al 1981. Ann. Ist. Univ. Nav. LI, 1–58.

De Maio, A., Moretti, M., Sansone, E., Spezie, G., Vultaggio, M., 1985. Outline of marine currents in the Bay of Naples and some considerations on pollutant transport. Nuovo Cimento 8C, 955–969.

Di Lorenzo, E., 2003. Seasonal dynamics of the surface circulation in the Southern California Current System. Deep-Sea Res. II 50, 2371–2388.

Dinniman, M.S., Klinck, J.M., Smith Jr., W.O., 2003. Cross-shelf exchange in a model of the Ross Sea circulation and biogeochemistry. Deep-Sea Res. II 50, 3103–3120.

Erofeeva, S.Y., Egbert, G.D., Kosro, P.M., 2003. Tidal currents on the central Oregon shelf: models, data, and assimilation. J. Geophys. Res. 108, 3148.

Fairall, C.W., Bradley, E.F., Rogers, D.P., Edson, J.B., Young, G.S., 1996. Bulk parameterization of air-sea fluxes for Tropical Ocean-Global Atmosphere Coupled-Ocean Atmosphere Response Experiment. J. Geophys. Res. 101, 3747–3764.

Gough, M.K., Garfield, N., McPhee-Shaw, E., 2010. An analysis of HF radar measured surface currents to determine tidal, wind-forced, and seasonal circulation in the Gulf of the Farallones, California, United States. J. Geophys. Res. 115, C04019.

Gravili, D., Napolitano, E., Pierini, S., 2001. Barotropic aspects of the dynamics of the Gulf of Naples (Tyrrhenian Sea). Cont. Shelf Res. 21, 455–471.

Grieco, L., Tremblay, L.-B., Zambianchi, E., 2005. A hybrid approach to transport processes in the Gulf of Naples: an application to phytoplankton and zooplankton population dynamics. Cont. Shelf Res. 25, 711–728.

Gurgel, K.-W., Essen, H.-H., Kingsley, S.P., 1999. High-frequency radars: physical limitations and recent developments. Coast. Eng. 37, 201–218.

Haidvogel, D.B., Arango, H.G., Hedstrom, K., Beckmann, A., Malanotte-Rizzoli, P., Shchepetkin, A.F., 2000. Model evaluation experiments in the North Atlantic Basin: simulations in nonlinear terrain-following coordinates. Dyn. Atmos. Oceans 32, 239–281.

Iermano, I., Liguori, G., Iudicone, D., Buongiorno Nardelli, B., Colella, S., Zingone, A., Saggiomo, V., Ribera d'Alcalà, M., 2012. Filament formation and evolution in buoyant coastal waters: observation and modelling. Prog. Oceanogr. 106, 118–137.

Jolliffe, I.T., 2002. Principal Component Analysis — Second Edition. Springer–Verlag, New York.

Kallos, G., Nickovic, S., Papadopoulos, A., Jovic, D., Kakaliagou, O., Misirlis, N., Boukas, L., Mimikou, N., Sakellaridis, G., Papageorgiou, J., Anadranistakis, E., Manousakis, M., 1997. The Regional Weather Forecasting System Skiron: An Overview. Proceedings of the Symposium on Regional Weather Prediction on Parallel Computer Environments, pp. 109–122 (15–17 October 1997, Athens, Greece).

Kaplan, D.M., Largier, J., Botsford, L.W., 2005. HF radar observations of surface circulation off Bodega Bay (northern California, USA). J. Geophys. Res. 110, C10020.

Koch, A.O., Kurapov, A.L., Allen, J.S., 2010. Near-surface dynamics of a separated jet in the coastal transition zone off Oregon. J. Geophys. Res. 115, C08020.

Kosro, P.M., 2005. On the spatial structure of coastal circulation off Newport, Oregon, during spring and summer 2001 in a region of varying shelf width. J. Geophys. Res. 110, C10S06.

Kosro, P.M., Barth, J.A., Strub, P.T., 1997. The coastal jet: observations of surface currents over the Oregon Continental Shelf from HF Radar. Oceanography 10, 53–56.

Kovačević, V., Gačić, M., Mancero Mosquera, I., Mazzoldi, A., Marinetti, S., 2004. HF radar observations in the northern Adriatic: surface current field in front of the Venetian Lagoon. J. Mar. Syst. 51, 95–122.

Krivosheya, V.G., Ovchinnikov, I.M., 1973. Peculiarities in the geostrophic circulation of the waters of the Tyrrhenian Sea. Oceanology 13, 822–827.

Kuang, L., Blumberg, A.F., Georgas, N., 2012. Assessing the fidelity of surface currents from a coastal ocean model and HF radar using drifting buoys in the Middle Atlantic Bight. Ocean Dyn. 62, 1229–1243.

Kurapov, A.L., Egbert, G.D., Allen, J.S., Miller, R.N., Erofeeva, S.Y., Kosro, P.M., 2003. The M_2 internal tide off Oregon: inferences from data assimilation. J. Phys. Oceanogr. 33, 1733–1757.

Marino, D., Modigh, M., Zingone, A., 1984. General features of phytoplankton communities and primary production in the Gulf of Naples and adjacent waters. In: Holm-Hansen, O., Bolis, L., Gilles, R. (Eds.), Marine Phytoplankton Productivity. Lecture Notes on Coastal and Estuarine Studies. Springer, Berlin, pp. 89–100.

Mazzocchi, M.G., Licandro, P., Dubroca, L., Di Capua, I., Saggiomo, V., 2011. Zooplankton associations in a Mediterranean long-term time-series. J. Plankton Res. 33, 1163–1181.

Mazzocchi, M.G., Dubroca, L., García Comas, C., Di Capua, I., Ribera d'Alcalà, M., 2012. Stability and resilience in coastal copepod assemblages: the case of the Mediterranean long-term ecological research at Station MC (LTER-MC). Prog. Oceanogr. 97–100 (135–151).

Menna, M., Mercatini, A., Uttieri, M., Buonocore, B., Zambianchi, E., 2007. Wintertime transport processes in the Gulf of Naples investigated by HF radar measurements of surface currents. Nuovo Cimento 30 C, 605–622.
Millot, C., 1987. Circulation in the western Mediterranean Sea. Oceanol. Acta 10, 149-149.
Molcard, A., Poulain, P.M., Forget, P., Griffa, A., Barbin, Y., Gaggelli, J., De Maistre, J.C., Rixen, M., 2009. Comparison between VHF radar observations and data from drifter clusters in the Gulf of La Spezia (Mediterranean Sea). J. Mar. Syst. 78 (Supplement), S79–S89.
Montuori, P., Triassi, M., 2012. Polycyclic aromatic hydrocarbons loads into the Mediterranean Sea: estimate of Sarno River inputs. Mar. Pollut. Bull. 64, 512–520.
Moretti, M., Sansone, E., Spezie, G., Vultaggio, M., De Maio, A., 1976–1977. Alcuni aspetti del movimento delle acque del Golfo di Napoli. Ann. Ist. Univ. Nav. XLV–XLVI, 207–217.
Navarra, A., Simoncini, V., 2010. A Guide to Empirical Orthogonal Functions for Climate Data Analysis. Springer, Dordrecht.
O'Keefe, S., 2005. Observing the Coastal Ocean with HF Radar. MS Thesis. Oregon State University.
Paduan, J.D., Cook, M.S., 1997. Mapping surface currents in Monterey Bay with CODAR-type HF radar. Oceanography 10, 49–52.
Paduan, J.D., Graber, H.C., 1997. Introduction to high-frequency radar: reality and myth. Oceanography 10, 36–39.
Paduan, J.D., Rosenfeld, L.K., 1996. Remotely sensed surface currents in Monterey Bay from shore-based HF radar (CODAR). J. Geophys. Res. 101 (C9), 20669–20686.
Paduan, J.D., Shulman, I., 2004. HF radar data assimilation in the Monterey Bay area. J. Geophys. Res. 109, C07S09.
Paduan, J.D., Washburn, L., 2013. High-frequency radar observations of ocean surface currents. Ann. Rev. Mar. Sci. 5, 115–136.
Pierini, S., Simioli, A., 1998. A wind-driven circulation model of the Tyrrhenian Sea area. J. Mar. Syst. 18, 161–178.
Ribera d'Alcalà, M., Conversano, F., Corato, F., Licandro, P., Mangoni, O., Marino, D., Mazzocchi, M.G., Modigh, M., Montresor, M., Nardella, N., Saggiomo, V., Sarno, D., Zingone, A., 2004. Seasonal patterns in plankton communities in a pluriannual time series at a coastal Mediterranean site (Gulf of Naples): an attempt to discern recurrences and trends. Sci. Mar. 68 (Suppl. 1), 65–83.
Rinaldi, E., Buongiorno Nardelli, B., Zambianchi, E., Santoleri, R., Poulain, P.-M., 2010. Lagrangian and Eulerian observations of the surface circulation in the Tyrrhenian Sea. J. Geophys. Res. 115, C04024.
Robinson, A.M., Wyatt, L.R., 2011. A two year comparison between HF radar and ADCP current measurements in Liverpool Bay. J. Oper. Oceanogr. 4, 33–45.
Russo, A., Coluccelli, A., Iermano, I., Falcieri, F., Ravaioli, M., Bortoluzzi, G., Focaccia, P., Stanghellini, G., Ferrari, C.R., Chiggiato, J., Deserti, M., 2009. An operational system for forecasting hypoxic events in the northern Adriatic Sea. Geofizika 26, 191–213.
Serafino, F., Lugni, C., Ludeno, G., Arturi, D., Uttieri, M., Buonocore, B., Zambianchi, E., Budillon, G., Soldovieri, F., 2012. REMOCEAN: a flexible X-band radar system for sea-state monitoring and surface current estimation. IEEE Geosci. Remote Sens. Lett. 9, 822–826.
Shchepetkin, A.F., McWilliams, J.C., 2003. A method for computing horizontal pressure-gradient force in an oceanic model with a nonaligned vertical coordinate. J. Geophys. Res. 108, 3090.
Shchepetkin, A.F., McWilliams, J.C., 2005. The regional oceanic modeling system (ROMS): a split-explicit, free-surface, topography-following-coordinate oceanic model. Ocean Model. 9, 347–404.
Taylor, K.E., 2001. Summarizing multiple aspects of model performance in a single diagram. J. Geophys. Res. 106, 7183–7192.
Tornero, C., Ribera d'Alcalà, M., 2014. Contamination by hazardous substances in the Gulf of Naples and nearby coastal areas: a review of sources, environmental levels and potential impacts in the MSFD perspective. Sci. Total Environ. 466–467 (820–840).
Umlauf, L., Burchard, H., 2003. A generic length-scale equation for geophysical turbulence models. J. Mar. Res. 61, 235–265.
Uttieri, M., Cianelli, D., Buongiorno Nardelli, B., Buonocore, B., Falco, P., Colella, S., Zambianchi, E., 2011. Multiplatform observation of the surface circulation in the Gulf of Naples (Southern Tyrrhenian Sea). Ocean Dyn. 61, 779–796.
Warner, J.C., Sherwood, C.R., Arango, H.G., Signell, R.P., 2005a. Performance of four turbulence closure models implemented using a generic length scale method. Ocean Model. 8, 81–113.
Warner, J.C., Geyer, W.R., Lerczak, J.A., 2005b. Numerical modeling of an estuary: a comprehensive skill assessment. J. Geophys. Res. 110, C05001.
Wilkin, J.L., Arango, H.G., Haidvogel, D.B., Lichtenwalner, C.S., Glenn, S.M., Hedström, K.S., 2005. A regional ocean modeling system for the Long-term Ecosystem Observatory. J. Geophys. Res. 110, C06S91.
Zingone, A., Montresor, M., Marino, D., 1990. Summer phytoplankton physiognomy in coastal waters of the Gulf of Naples. Mar. Ecol. 11, 157–172.
Zingone, A., Casotti, R., Ribera d'Alcalà, M., Scardi, M., Marino, D., 1995. 'St Martin's summer': the case of an autumn phytoplankton bloom in the Gulf of Naples (Mediterranean Sea). J. Plankton Res. 17, 575–593.
Zingone, A., Dubroca, L., Iudicone, D., Margiotta, F., Corato, F., Ribera d'Alcalà, M., Saggiomo, V., Sarno, D., 2010. Coastal phytoplankton do not rest in winter. Estuar. Coasts 33, 342–361.